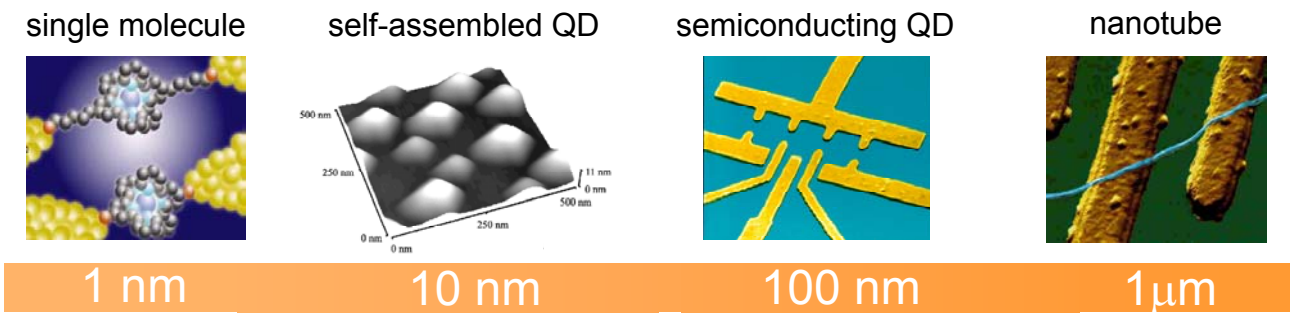

Figure 1. Different quantum dot systems.

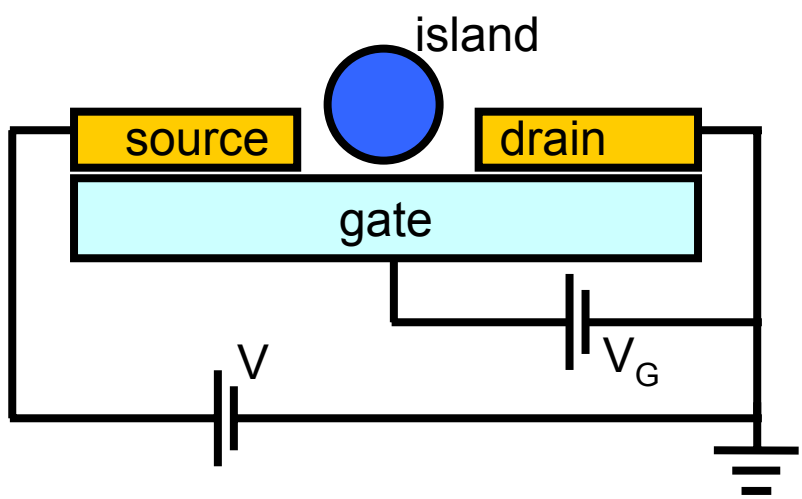

Figure 2. Schematic drawing of the three-terminal device lay-out.

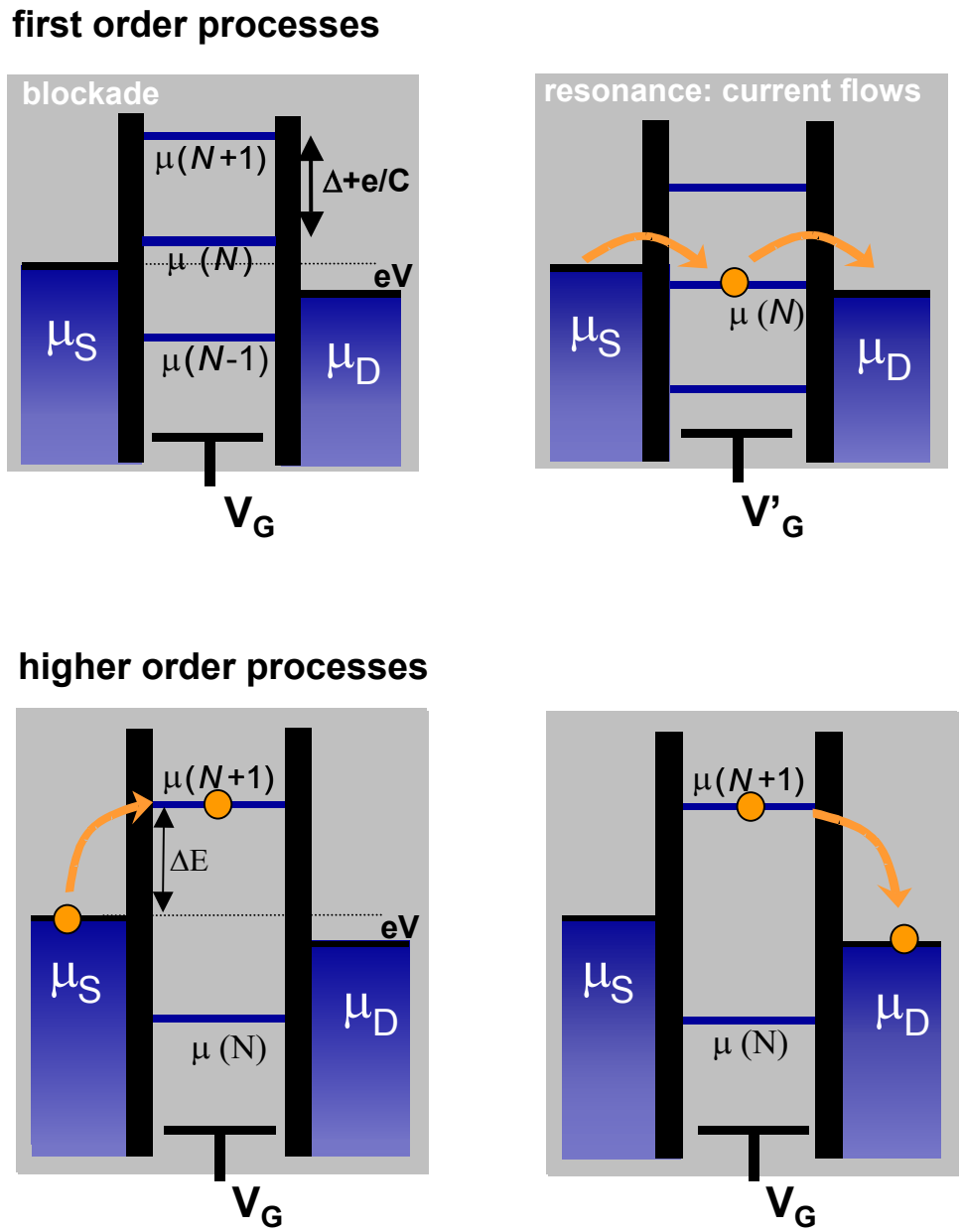

Figure 3. Schematic drawing of the electrochemical potentials of an island connected to two reservoirs, across which a small (negative) bias voltage V is applied. A voltage on the gate electrode can be used to shift the electrostatic potential of the energy level. Top: resonant transport becomes possible when the gate voltage pushes one of the levels within the bias window eV. The $\mu(N)$ level is aligned with μ_S and the number of electrons on the dot alternates between N and N-1 (sequential tunneling). Bottom: the levels are not aligned. Coulomb blockade fixes the number of electrons on the dot to N. Transport, however, is possible through a virtual co-tunnel process in which a unoccupied level is briefly occupied. A similar process exists for the occupied level, $\mu(N)$, which can be briefly unoccupied. In contrast to resonant transport the level is empty (full) most of the time. For all panels one should note that in reality, the levels are not sharp lines but they have a finite width Γ. Similarly, the edge between the occupied (blue) and unoccupied states is blurred by temperature via the Fermi-Dirac function.

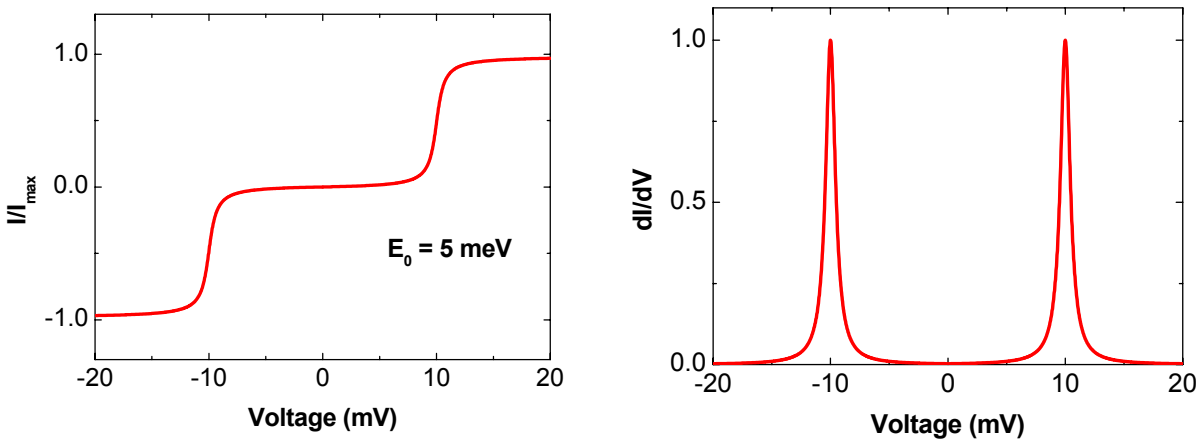

Figure 4. Left: current-voltage characteristic calculated with Eq. 6 for a level that is located 5 meV from the nearest Fermi energy of one of the electrodes. A symmetric coupling to the leads is assumed with a total broadening of 0.5 meV. Right: corresponding differential conductance with a peak height equal to the conductance quantum. Note that the peak width is of the order of the total broadening.

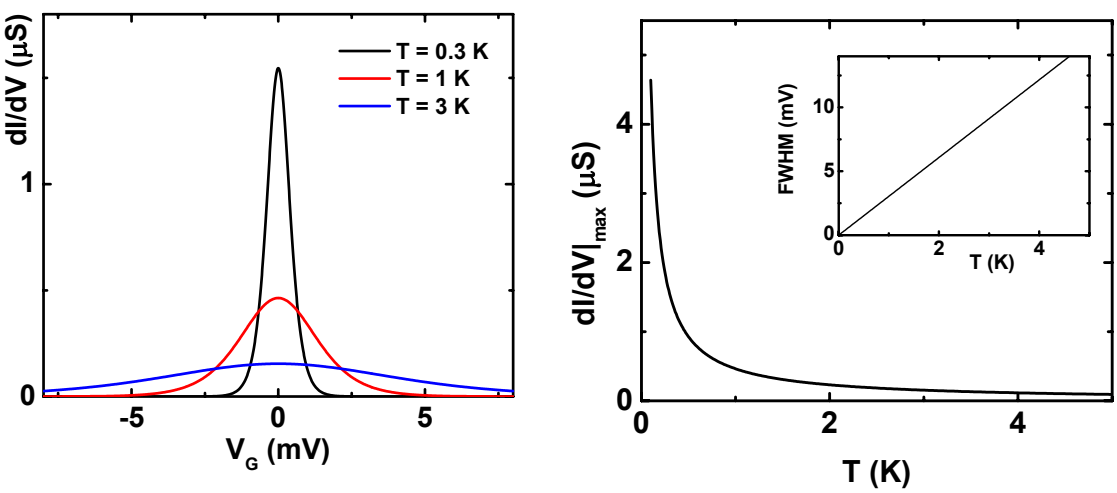

Figure 5. Left: Temperature dependence of the Coulomb peak height (Eq. 9) in the resonant transport model showing the characteristic increase as temperature is lowered. Right: peak height as a function of temperature. The inset shows the full width half maximum (FWHM) of the Coulomb peak as a function of temperature (see text). Calculations are performed with $\Gamma = 10^9$ 1/s and a gate coupling of 0.1 in the regime $\Gamma < k_B T$.

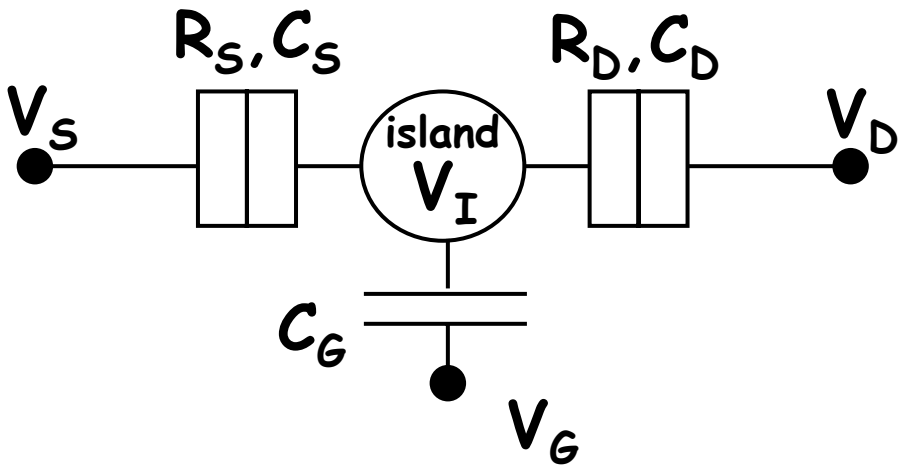

Figure 6. Capacitance model. Schematic drawing of an island connected to source and drain electrodes with tunnel junctions; the gate electrode shifts the electrostatic potential of the island.

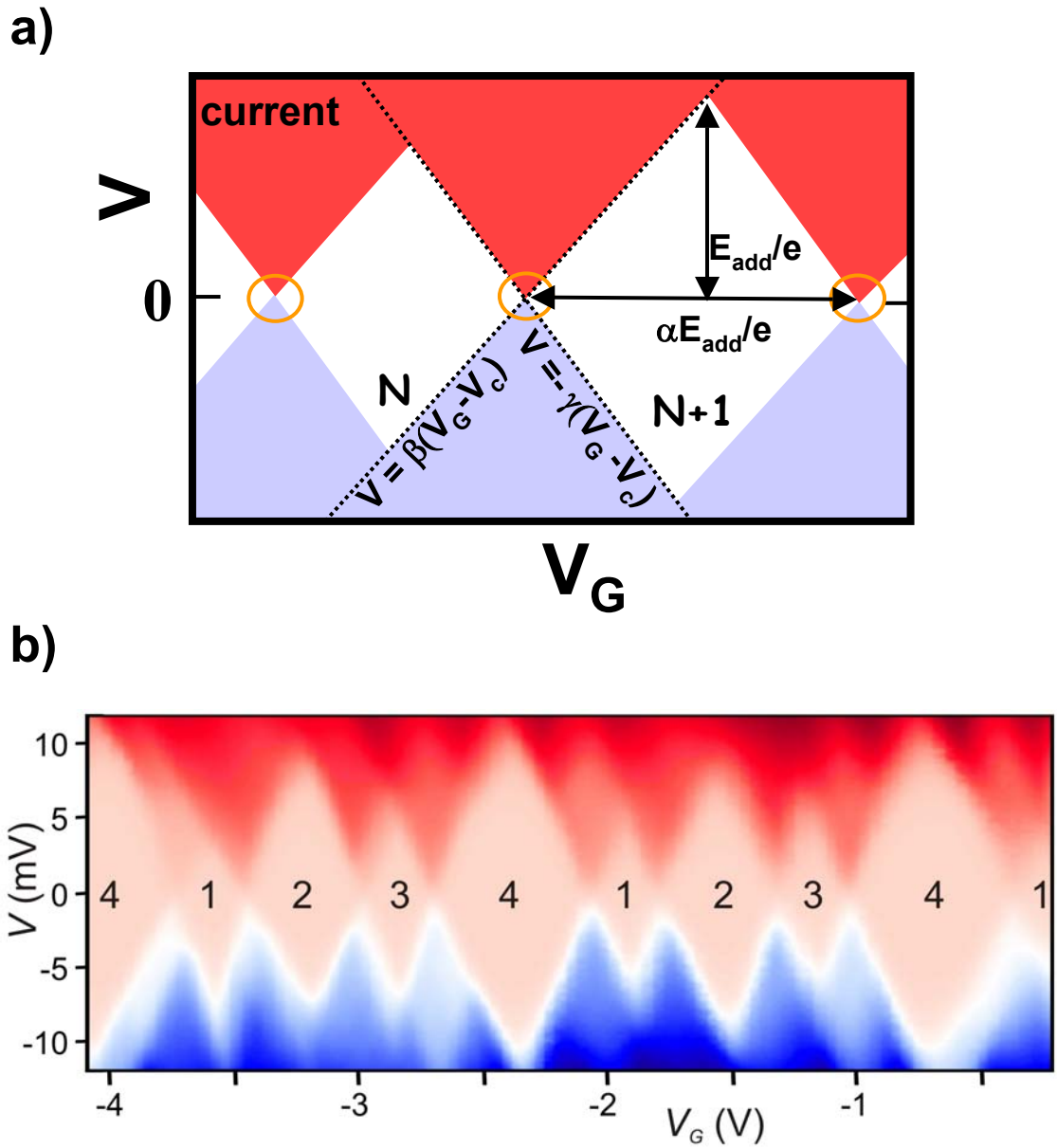

Figure 7. Linear transport. a) Two-dimensional plot of the current as a function of bias and gate voltage (stability diagram). For small bias current only flows in the three point corresponding to the situation drawn in Fig. 3 top right. These points are called the degeneracy points. Red: positive currents. Blue: negative currents. White: blockade, no current. b) Measured stability diagram of a metallic single-walled carbon nanotube showing the expected fourfold shell filling. Blockade regime is pink. Data taken from Ref. [5].

a)

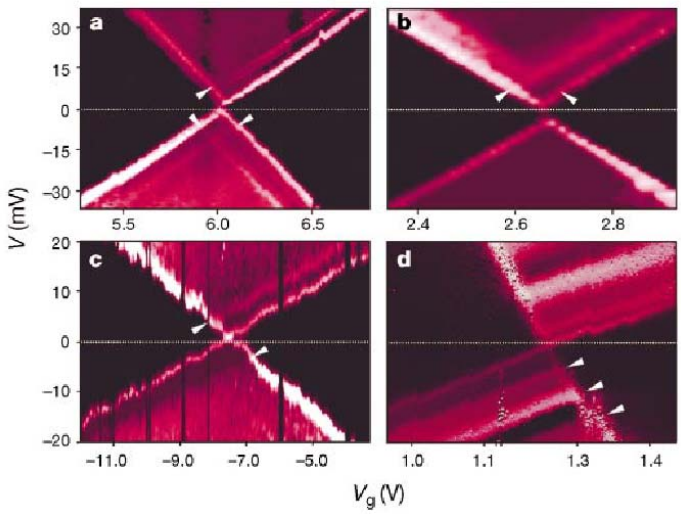
a
b
c
d
30
15
0
−15
−30
V (mV)
5.5
6.0
6.5
2.4
2.6
2.8
20
10
0
−10
−20
−11.0
−9.0
−7.0
−5.0
1.0
1.1
1.3
1.4
V_g (V)

b)

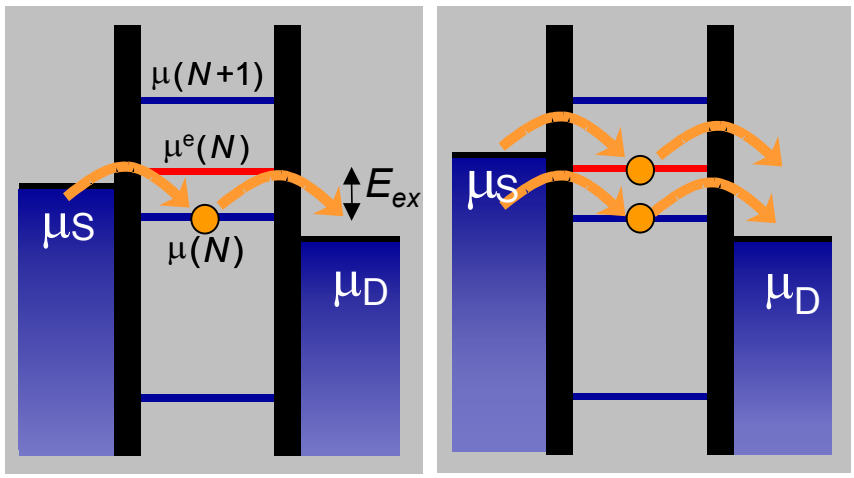
μ(N+1)
μ^e(N)
μ(N)
μS
μD
E_ex
μS
μD

c)

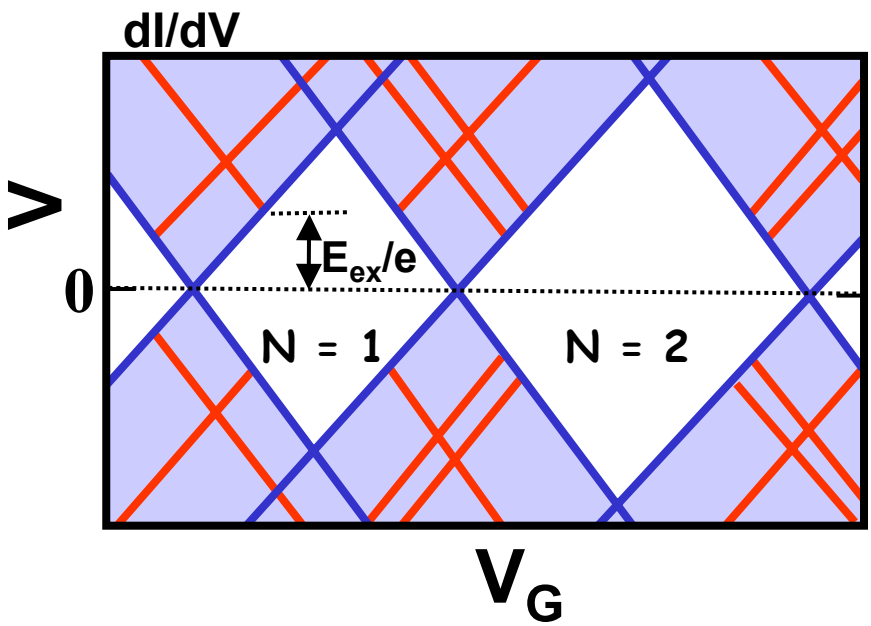
dI/dV
V
0
E_ex/e
N = 1
N = 2
V_G

Figure 8. Non-linear transport and excited states. a) Four different conductance maps (stability diagrams) of C_{60} molecules trapped between two electrodes [7]. Excitations indicated by arrow heads and running parallel to the diamond edges are due to vibrational modes of the C_{60} molecule. b) Electrochemical potential plot of a dot with three electronic energy levels and one excited state (red). Transport through an excited level becomes possible as soon as the red level enters the bias window. c) Schematic of a differential conductance map. Red lines show the positions at which excited states enter the bias window. The associated step-wise increases in current show up as a lines running parallel to the edges of the diamond-shaped regions. Blue: dI/dV is zero but the current is not (sequential-tunneling regime). White: current blockade.

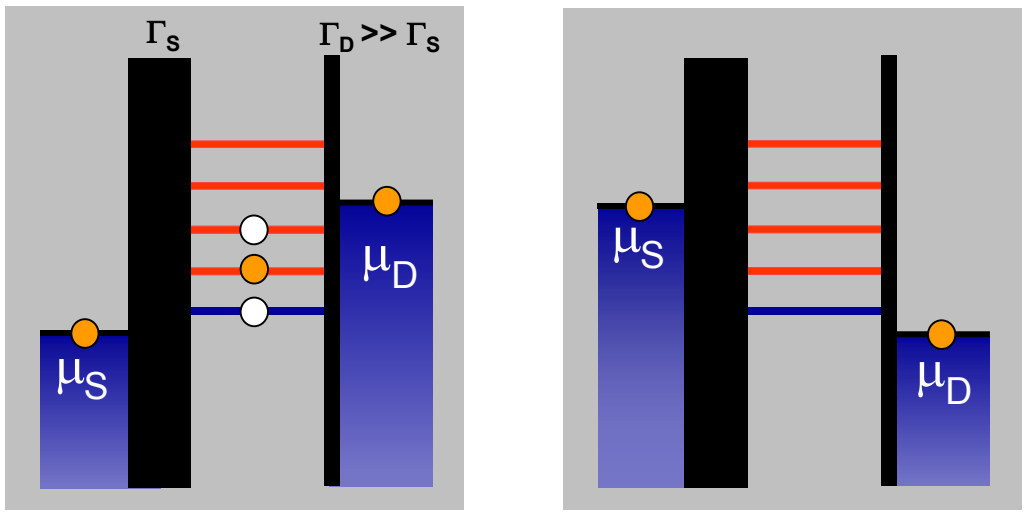

Figure 9. Asymmetric coupling to the electrodes leads to an almost full occupancy if tunneling out of the level is limited by the thick barrier (left: low tunnel rate in) and almost zero occupancy of the level if tunnelling out is determined by the thin barrier (right: high tunnel rate in). Note, that of the three levels in the bias window only one of them can be occupied at the same time. An increase of the bias voltage such that another excited level enters the bias window yields a very small current increase in the case depicted on the left hand side because the thick barrier remains the limiting factor for the current. In the right hand side on the other hand a new transport channel becomes available and the current shows a clear step-wise increase.

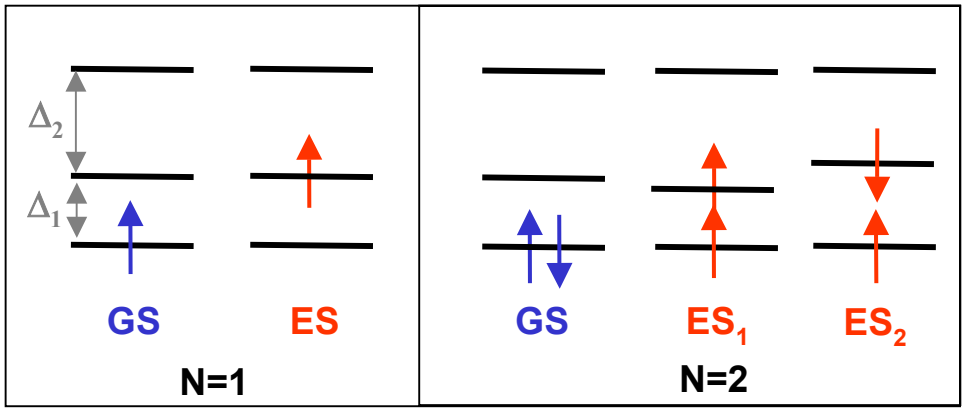

Figure 10. Schematic drawing of the ground state (GS) filling and the excited states (ES). Left: the island contains one electron and the first excited state involves a transition to the nearest unoccupied level. (In zero magnetic field there is an equal probability to find a down spin on the dot.) Right: two electrons with opposite spin occupy the lowest level. The first excited state involves the promotion of one of the spins to the nearest unoccupied level. A ferromagnetic favors a spin flip. The antiparallel configuration (ES_2) has a higher energy (see text).

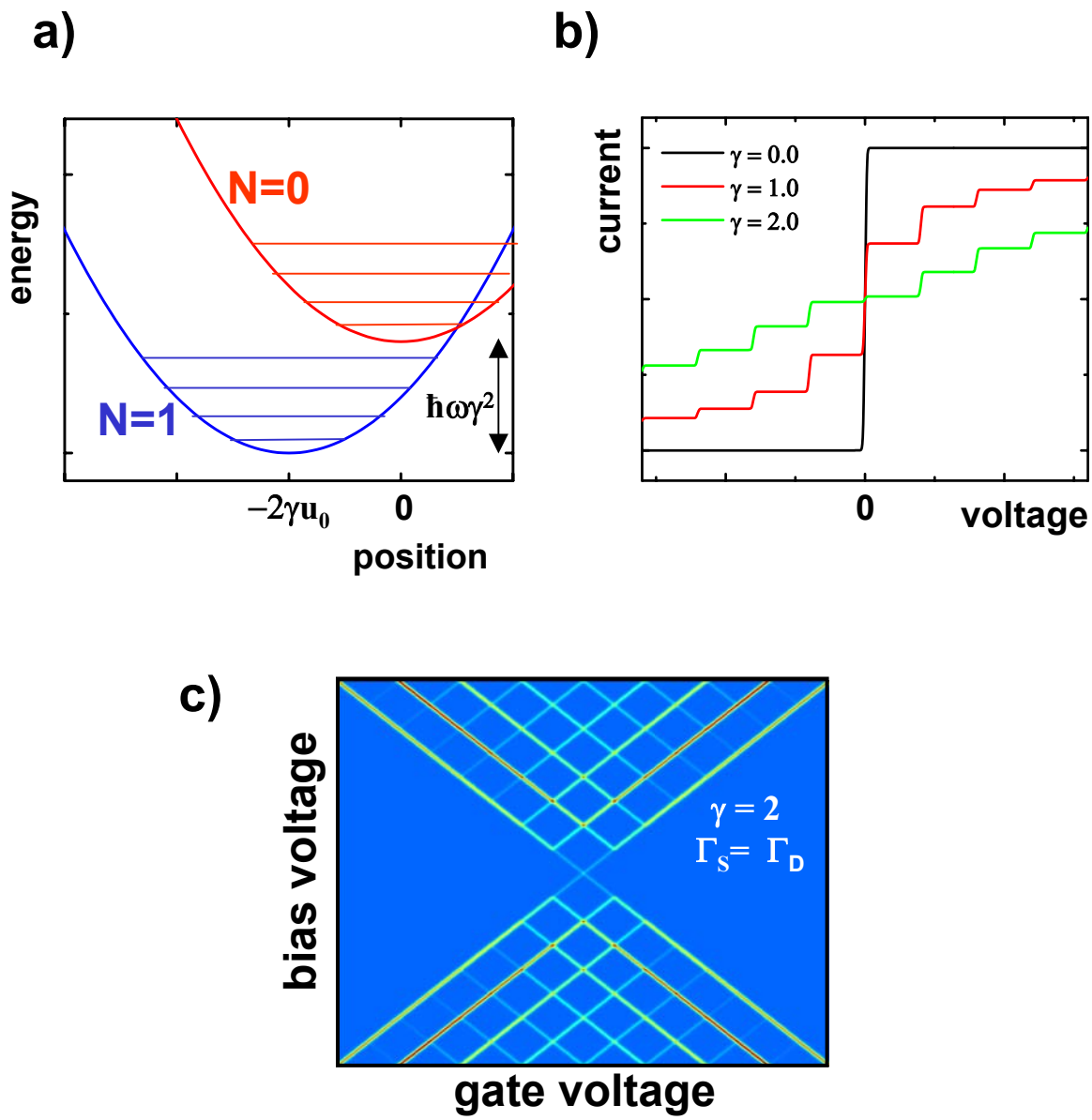

Figure 11. a) Potential of the harmonic oscillator for the empty (red) and occupied state (blue). When an electron tunnels onto the island, the position of the potential minimum is shifted in space and energy. b) Current-voltage characteristics calculated for three different values of the electron-phonon coupling constant. For nonzero coupling steps appear, which are equally spaced in the voltage (harmonic spectrum). c) Differential conductance plotted in a stability diagram for an island coupled to a single vibrational mode. Lines running parallel to the diamond edges correspond to the steps in b). Around zero bias the current is suppressed for this rather large e-ph coupling (phonon blockade).

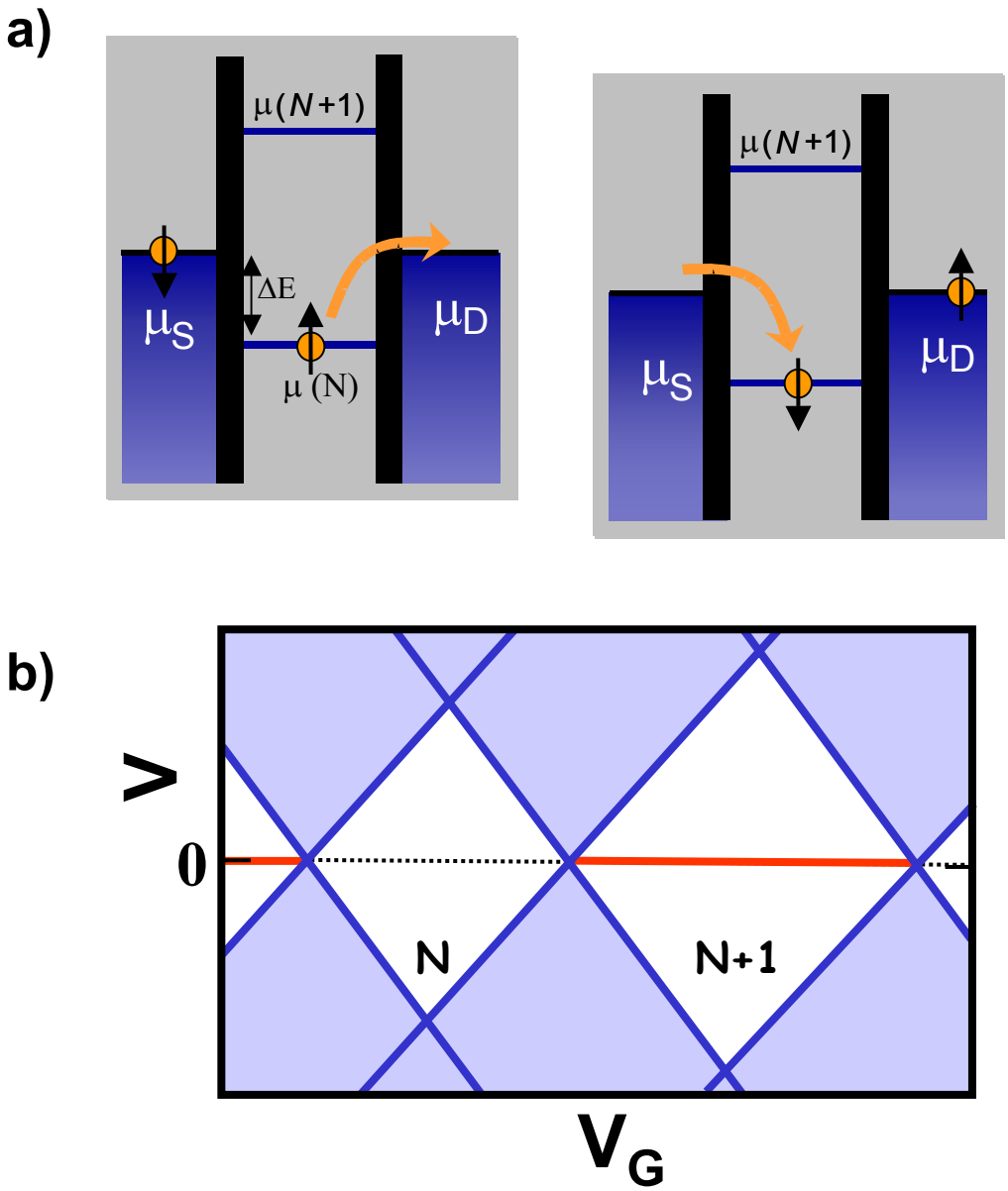

Figure 12. a) Schematic drawing of the two-step Kondo process which occurs for odd occupancy of the island. Bb) shows how the Kondo effect and leads to a zero bias conductance peak (red lines) in the differential conductance plots.

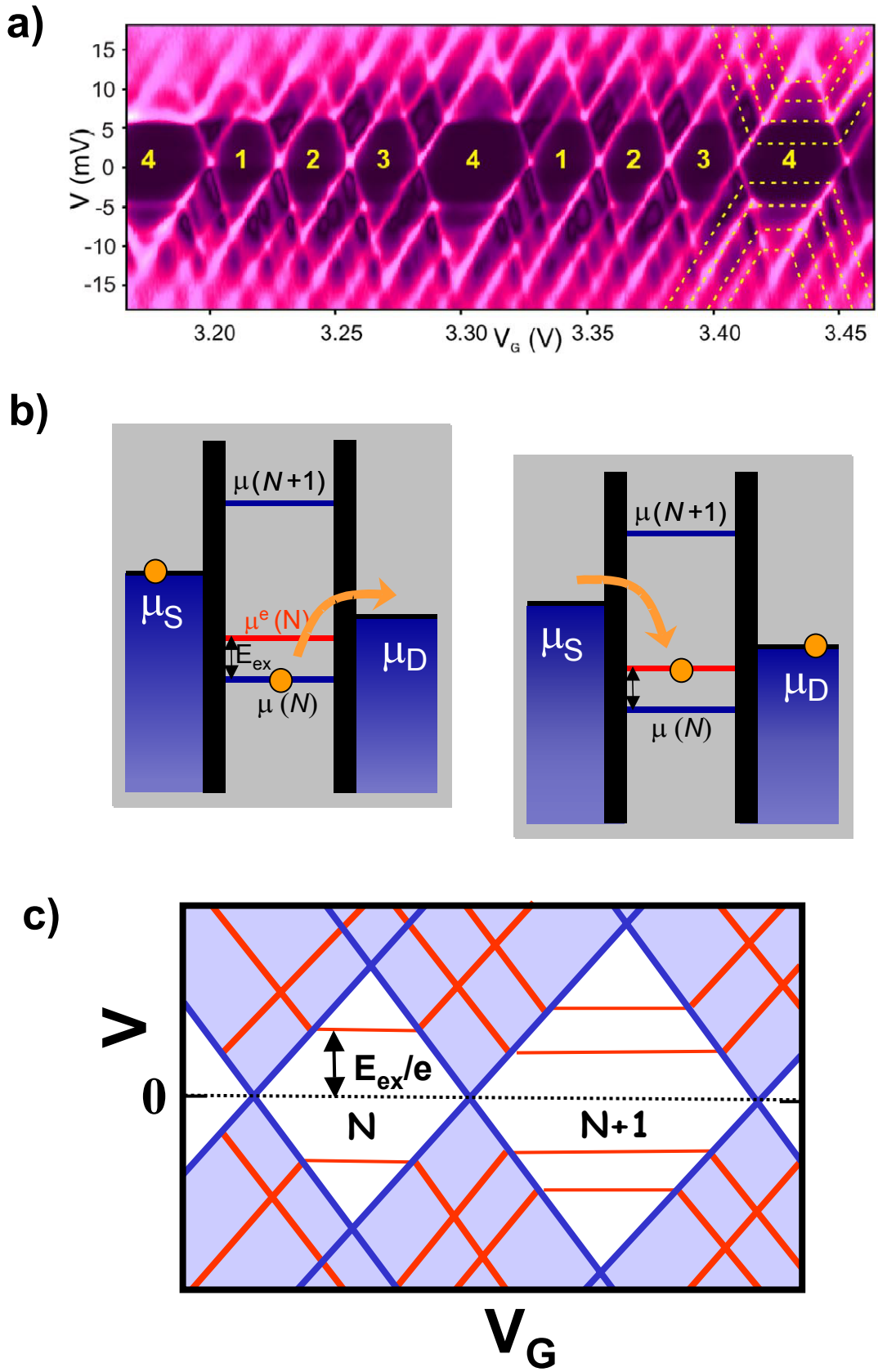

Figure 13. Inelastic co-tunneling. a) Measured stability diagram of a metallic single-walled carbon nanotube (taken from Ref. [5]). Dashed horizontal lines indicate the presence of inelastic co-tunnel lines. b) Schematic drawing of this two-step tunneling process, leaving the dot in an excited state. c) Inelastic co-tunneling gives rise to horizontal lines in the blocked current region. The energy of the excitation can directly be determined from these plots as indicated in the figure.